

Published in final edited form as:

Cryst Growth Des. 2011 April 6; 11(4): 1182–1192. doi:10.1021/cg101384p.

Membrane Protein Crystallization in Lipidic Mesophases. Hosting lipid affects on the crystallization and structure of a transmembrane peptide

Nicole Höfer^{†,‡}, David Aragão[†], Joseph A. Lyons^{†,‡}, and Martin Caffrey^{†,*}

[†]Membrane Structural and Functional Biology Group, School of Biochemistry and Immunology, and School of Medicine, Trinity College, Dublin [‡]Department of Chemical and Environmental Sciences, University of Limerick, Limerick, Ireland

Abstract

Gramicidin is an apolar pentadecapeptide antibiotic consisting of alternating D- and L-amino acids. It functions, in part, by creating pores in membranes of susceptible cells rendering them leaky to monovalent cations. The peptide should be able to traverse the host membrane either as a double stranded, intertwined double helix (DSDH) or as a head-to-head single stranded helix (HSSH). Current structure models are based on macromolecular X-ray crystallography (MX) and nuclear magnetic resonance (NMR). However, the HSSH form has only been observed by NMR. The shape and size of the different gramicidin conformations differ. We speculated therefore that reconstituting it into a lipidic mesophase with bilayers of different microstructures would preferentially stabilize one form over the other. By using such mesophases for *in meso* crystallogeneses the expectation was that at least one would generate crystals of gramicidin in the HSSH form for structure determination by MX. This was tested using commercial and in-house synthesised lipids that support *in meso* crystallogeneses. Lipid acyl chain lengths were varied from 14 to 18 carbons to provide mesophases with a range of bilayer thicknesses. Unexpectedly, all lipids produced high quality, structure-grade crystals with gramicidin only in the DSDH conformation.

1. Introduction

The lipidic cubic mesophase is proving to be a generally useful hosting medium in which to crystallize membrane proteins for diffraction-based structure determination (www.mpdb.tcd.ie).^{1,2} The cubic phase is a lyotropic liquid crystal. It consists of a highly curved lipid bilayer the mid-plane of which is draped over a periodic minimal surface with cubic symmetry.³ The bilayer separates two interpenetrating but non-contacting aqueous channels. Both the aqueous and bilayer compartments are continuous in three dimensions. As a result, the mesophase is described as being bicontinuous (Figure 1). Crystallogeneses in the lipidic cubic mesophase, by the so-called '*in meso*' method, begins with a reconstitution of the target protein into the bilayer. Precipitants, added to trigger nucleation and crystal

*Corresponding Author Membrane Structural and Functional Biology Group, School of Biochemistry and Immunology and School of Medicine, Trinity College Dublin, Dublin 2, Ireland, Phone: 353-1-896-4253; Fax: 353-1-896-4253, martin.caffrey@tcd.ie, Web addresses: www.tcd.ie.

SUPPORTING MATERIAL

Materials and Methods and additional references are available at ?

ACCESSION NUMBER

Coordinates and structure factors have been deposited in the Protein Data Bank under identification codes 2Y5M, PDB ID and 2XDC.

growth, have been proposed to stabilize a local planar phase within the mesophase. The protein preferentially partitions into and concentrates in these lamellar domains in a process that culminates in nucleation and crystal growth.⁴

The *in meso* method works with a variety of membrane protein types. These range from multi-subunit complexes all the way to short, integral membrane polypeptides. Given that crystallization takes place in the context of a bilayered membrane the expectation is that the target protein is in a stable, native conformation prior to entering the ordered lattice of a crystal. This suggests that it might be possible to tailor the state of the protein by adjusting the characteristics of the hosting bilayer and to capture particular conformations in the crystal that forms under *in meso* conditions. This idea was investigated in the current study using the integral membrane peptide, gramicidin.

Linear gramicidin is a highly apolar pentadecapeptide antibiotic consisting of alternating D- and L-amino acids. It is produced non-ribosomally by *Bacillus brevis* and functions, in part, by creating pores in membranes of susceptible cells rendering them leaky to monovalent cations. Naturally occurring gramicidin (gD) is a mixture of isoforms: gA (80%), gB (6%), and gC (14%). The amino acid sequence of gA is: formyl-NH-L-Val-Gly-L-Ala-D-Leu-L-Ala-D-Val-L-Val-D-Val-L-Trp-D-Leu-L-Trp-D-Leu-L-Trp-D-Leu-L-Trp-CO-NH-CH₂-CH₂-OH. In gB and gC, Trp at position 11 (underlined) is replaced by L-Phe and L-Tyr, respectively.⁶ The ion conducting form of gD is generally considered to be a dimer. Controversy exists as to whether this is a head-to-head, single stranded helical dimer (HSSH)⁷ or a left- or right-handed intertwined, parallel or antiparallel, double stranded double helix (DSDH)⁸⁻¹⁰. The peptide should be able to traverse its hosting membrane as either a DSDH or HSSH (Figure 2).

Current structure models of gramicidin are based on macromolecular X-ray crystallography (MX) and nuclear magnetic resonance (NMR) (Table 1). However, the HSSH form has only been observed by NMR.

The shape and dimensions of the different gramicidin conformations can differ (Figure 2). We speculated therefore that reconstituting gramicidin into a lipidic mesophase with bilayers of different thicknesses would preferentially stabilize one form over the other. By using such mesophases for *in meso* crystallogenesis, the expectation was that at least one would generate crystals of gramicidin in the HSSH form for structure determination by MX.

The hypothesis was tested using commercial and in-house synthesized monoacylglycerols (MAGs) that support *in meso* crystallogenesis. Lipid acyl chain lengths were varied from 14 to 18 carbons to provide mesophases with a range of bilayer thicknesses. All lipids produced high quality, diffraction-grade crystals and structures with resolution in the range from 1.08 to 1.70 Å. Surprisingly, regardless of the lipid identity only the DSDH conformation was observed.

2. Materials and Methods

2.1. Materials

Monoolein (9.9 MAG, Footnote 1, Lots: M-239-A21-Q, M-239-516-5, 356 g/mol) was obtained from NuChek Prep Inc. (Elysian, MN, USA). Linear gramicidin D (Lot: 1345609 13307134, 1,880 g/mol) and 2,2,2-trifluoroethanol (TFE, Lot: S25895-495) were purchased from Sigma-Aldrich (Dublin, Ireland). The lipids 7.7 MAG (Lots: JPL-4-92, JL-3-68, 300 g/mol) and 8.8 MAG (Lot: JPL-2-42, 328 g/mol) were synthesized and purified in-house following established procedures.^{21,22} PEG/Ion (Lot: 212629), Index (Lot: 214407), Crystal Screen I (Lot: 211094), Crystal Screen II (Lot: 211251) and MembFac (Lot: 211423)

crystallization screens were obtained from Hampton Research (Aliso Viejo, CA, USA). Wizard I, Wizard II, and Wizard III (Lot: EBS000322200499) were sourced from Emerald BioSystems, Inc. (Bainbridge Island, WA, USA). The crystallization screen MemStart (Lot: 011–121) was obtained from Molecular Dimensions (Suffolk, UK). PEG 400 (Lot: 0001418256) was purchased from Sigma-Aldrich (Dublin, Ireland). Water, with a resistivity of $>18 \text{ M}\Omega\cdot\text{cm}$, was purified using a Milli-Q Water System (Millipore, Bedford, MA, USA) consisting of an Elix 5 UV compartment (Lot: F4HN34349) with a Prograd@2 cartridge (Lot: F9HNO1157) to pre-purify water and a Synergy compartment (Lot: F4EN79695B) with a Simpак@1 cartridge (Lot: F9HN06031) to produce highly purified water followed by sterile filtration through a $0.22 \mu\text{m}$ MilliPAK@40 filter (Lot: F5PN18060).

2.2. Solubility of Gramicidin in Precipitant Solutions Containing PEG

To determine the solubility of gramicidin in the precipitant solutions that yielded crystals, a 10 mg/mL stock solution of gramicidin in TFE was prepared. This solution was mixed with the relevant precipitant solutions using a volume ratio of 1 part gramicidin solution to 9 parts precipitant solution and shaken by hand for 5 min at room temperature (RT, $18 - 23 \text{ }^\circ\text{C}$). The precipitate, which formed in all cases, was removed by centrifugation at $16,300 \times g$ for 5 min at RT. Absorbance of the supernatant was measured at 280 nm (A_{280}) and converted to peptide concentration using a measured extinction coefficient of $18,590 \text{ M}^{-1}\text{cm}^{-1}$. The latter was determined from the slope of an A_{280} versus gramicidin concentration curve established with the peptide dissolved in a solution composed of TFE, PEG 400, and water in the volume ratio 2:9:9.

2.3. Gramicidin/Lipid Mixture Preparation

Lipids and gramicidin were combined in a molar ratio of 20:1 followed by co-solubilization in 4 to 5 mL TFE in a 15 mL glass vial. Typically, between 50 and 100 mg of MAG were prepared with the appropriate amount of gramicidin. The solution was shaken by hand for approximately 3 min at RT until optically clear. TFE was removed by evaporation under a stream of nitrogen gas followed by high vacuum drying (10 mbar, Büchi Vac@ V500, Büchi, Flawil, Switzerland) at RT for 24 h.²³ Samples were stored at RT in the dark under nitrogen for a maximum of one week.

2.4. Cubic Phase Preparation

The cubic mesophase was prepared by combining the dry gramicidin/MAG mixture with Milli-Q water in coupled 0.1 mL gas-tight RN type syringes (Hamilton Company, Reno, Nevada, USA) at different weight ratios depending on the lipid, as previously described.^{24,25} Specifically, lipid:water weight ratios of 1:1, 1:1 and 3:2 were used for 7.7, 8.8 and 9.9 MAG, respectively.

2.5. *In meso* Crystallization

Crystallization trials were set up in 96-well glass sandwich plates using 50 nL mesophase and 800 nL precipitant solution with an *in meso* robot, as previously described.^{25,26} Plates were stored in an incubator/imager (RockImager RI1500, Formulatrix, Inc., Waltham, MA,

Footnote 1: The *in meso* crystallogenesi s reported on herein makes use of MAGs containing *cis* - monounsaturated fatty acids. A shorthand system for describing the chemical constitution of these lipids is referred to as the N.T MAG notation.⁵² This is based on a simplistic view of the MAG molecule as an object consisting of a head, a neck, and a tail with the latter two joined by a trunk. Here the head of the MAG is the glycerol head group. It is in ester linkage to the neck corresponding to that part of the acyl chain extending from its carboxyl carbon to the first carbon of the olefin. The trunk is the *cis* - double bond. The tail extends from the second carbon of the olefin to the chain's methyl terminus. In the N.T MAG notation, N and T correspond to the number of carbon atoms in the neck and tail, respectively. The total number of carbon atoms in the chain is the sum of N and T. Thus, 11.7 MAG represents monovaccenin, a MAG with a fatty acyl chain 18 carbon atoms long where the *cis* - double bond resides between carbon atoms 11 and 12. It is an olefinic isomer of 9.9 MAG commonly known as monoolein.

USA) at 20 °C. Crystals measuring $30 \times 30 \times 30 \mu\text{m}^3$ to $60 \times 60 \times 60 \mu\text{m}^3$ appeared after 3 to 5 days in a variety of precipitants, all of which contained PEG (Figure 3). Full details regarding the composition of the precipitant solutions that produced crystals for structure determination are reported in Table S1. Crystals, harvested using Cryo-loops (30 to 100 μm , Micro Mounts, MiTeGen, Ithaca, NY, USA), were directly cryo-cooled and stored in liquid nitrogen.²⁶

2.6. Data Collection

Diffraction data were collected at the General Medicine and Cancer Institutes Collaborative Access Team (GM/CA CAT) beamline 23ID-B at the Advanced Photon Source (APS) with a MAR 300 CCD detector using X-rays ranging from 0.827 to 1.033 Å (Table 2). Due to the small size of the crystals a minibeam of $10 \mu\text{m} \times 10 \mu\text{m}$ was used.²⁷ The crystals were kept cryo-cooled in a stream of nitrogen at 100 K during data collection with exposures of 1 to 2.3 s for each 1° or 2° oscillation. To ensure that all high-resolution reflections were collected the detector was moved to the minimum crystal-to-detector distance of 100 mm and the wavelength was set to 0.83 Å (data set 1, 7.7 MAG) and to 0.98 Å (data set 2, 8.8 MAG).

Data reduction was performed in HKL2000²⁸ and then converted to structure factors using the CCP4 program TRUNCATE²⁹. High resolution data were collected for data set 1 (7.7 MAG) with a highest resolution shell of 1.08 Å. Crystals for data set 2 (8.8 MAG) diffracted to 1.26 Å. For this lipid, a low resolution data set was collected and merged with two high resolution data sets. Crystals for data set 3 (9.9 MAG) diffracted to 1.70 Å. The same test set flag for R_{free} calculation assigned to data set 1 was carried over to data sets 2 and 3. All crystals were found to be in space group $P2_1$ with similar cell dimensions (Table 2). The asymmetric unit contained three dimers of gramicidin (total molecular weight, ~11.3 kDa) corresponding to a Matthews coefficient³⁰ of $2.6 \text{ \AA}^3 / \text{Da}$ and a solvent content of 52 %. Diffraction and refinement statistics are given in Table 2.

2.7. Phase Determination and Refinement

The phase problem for the highest resolution data set (data set 1, 7.7 MAG) was determined by molecular replacement with program Phaser³¹ using a poly-Ala pruned DSDH dimer (PDB entry 1AL4) and data truncated to 1.7 Å. Refinement was performed using restrained maximum likelihood as implemented in Refmac.³² Side chains were modelled in using Coot.³³ Positional and isotropic B-factor parameters were refined for each atom. Alternative conformations for side chains were added where suggested by $|\text{Fo}| - |\text{Fc}|$ maps with an initial occupancy of 0.5. In cases where B-factors and maps justified it, occupancy was set to 0.3 and to 0.7 so that maps were clear and neighbouring atoms had similar B-factors. After this stage of refinement, PEG, lipid, water molecules, and ions were added to the model based on electron density, standard geometrical and chemical restraints, and presence in the crystallization conditions. Molecules were subsequently deleted if they were not visible at the 1.0 sigma level in $2|\text{Fo}| - |\text{Fc}|$ electron density maps. Molecules assigned as PEG or lipid were also deleted if no clear hydrogen bonds could be assigned. Anisotropic B-factor refinement was then turned on followed by addition of hydrogens in riding positions and refined until convergence.

A similar structure determination and refinement protocol was followed for data set 2 (8.8 MAG) using as molecular replacement search model a poly-Ala version of the final, previously refined gramicidin dimer (2Y5M, 7.7 MAG). Structure determination and refinement for data set 3 (9.9 MAG) is described in Höfer et al.¹⁷

2.8. Structure Validation

The quality of the structural models was evaluated during the course of refinement using MolProbity,³⁴ RAMPAGE,³⁵ and Scheck³⁶. All programs show bond length and angle values as expected for structures at these resolutions. Ramachandran analysis³⁷ for each structure shows over 87 % of the residues in the most favoured regions, over 11 % of the residues in the allowed regions and no outliers (Table S2). These results are consistent with what is found for other gramicidin structures in the same conformation (see PDB entries 1AL4, 1ALZ, and 1ALX).⁹

The coordinates and structure factors for data set 1 (7.7 MAG), data set 2 (8.8 MAG) and data set 3 (9.9 MAG) have been deposited in the PDB under code identifiers: 2Y5M, PDB ID, and 2XDC, respectively.

3. Results and Discussion

3.1. Crystallization and Structure Determination

The purpose of this study was to determine if the character of the hosting mesophase, dictated by the lipid used to form it, would impact on the crystallization and structure of the transmembrane polypeptide, gramicidin. What we found was unexpected; the three lipids used to create the hosting mesophases for *in meso* crystallogenesis yielded identical crystals and identical structures for gramicidin. In all cases, the crystals grew to their full size within a week at room temperature with maximum dimensions in the 30 to 60 μm range. The space group in every instance was $P2_1$ with unit cell metrics of $a = c = 30.6 \text{ \AA}$, $b = 62.8 \text{ \AA}$, $\beta = 100.0^\circ$ to within error and the structures refined to reasonable R factors with good geometry (Section 2.8, Table 2). PEG was a common precipitant ingredient and was identified in the final crystal. For each of the three hosting lipids the phase from which crystals were harvested was of the sponge type.³⁸

The structure of gramicidin crystallized *in meso* in the three hosting lipids was solved initially by molecular replacement with a gramicidin model obtained using crystals grown from n-propanol.⁹ The *in meso* and n-propanol structures are remarkably similar. The peptide exists as a left-handed, intertwined helical homodimer in an anti-parallel arrangement (right panel, Figure 2). The asymmetric unit consists of three dimers and each unit cell has a total of 6 dimers. The two monomers within a dimer can be viewed as β -strands that associate to form a two-stranded lath or ribbon stabilized by either 24 or 26 interstrand hydrogen bonds, depending on the dimer, typical of β -sheets. Because the sequence consists of alternating D- and L- residues side chains are on one side of the ribbon. Their bulk contributes to a curving of the ribbon and to the formation of a β -helix with ~ 5.6 residues per turn (a $\beta^{5.6}$ -helix). Individual dimers are approximately 35 \AA long and have an outer diameter of 18 \AA (Figure 2). The core of the dimers is sealed and thus incapable of accommodating ions. Dimers are arranged in layers with their long axis oriented approximately normal to the layer plane (Figure 4). This, so-called Type I or layered packing³⁹ is consistent with the proposed mechanism for crystallization *in meso* (Figure 1); it has been observed in all crystal structures obtained to date by the *in meso* method.¹

Crystals formed from the three different lipids have the same crystal packing and composition. For simplicity therefore the following discussion will refer primarily to the highest resolution structure (data set 1, 7.7 MAG). As noted, there are three dimers within an asymmetric unit of the gramicidin crystal. For purposes of discussion, the three will be referred to as dimers AB, CD and EF with monomers identified by individual letters. Within the asymmetric unit, the AB and CD dimers associate to form a V-shaped object. The pointed end of the V is created by the N-terminal ends of chain A and chain D that are in van der Waals contact. The angle of the V is 25° and its splayed end has the main chain of

chains A and D separated by 14 Å. In contrast, the long axis of dimers CD and EF are almost parallel with a dimer center-to-center separation of around 20 Å. Dimers CD and EF are almost identical with an RMSD in C_α atom positions of 0.03 Å. Small structural differences exist between dimer AB and dimers CD and EF as reflected in slightly higher RMSD values.

In addition to the peptide, each asymmetric unit within the *in meso* gramicidin crystal contains four molecules of PEG and two molecules of water. The four PEG molecules have different lengths and are located in distinct parts of the asymmetric unit. The longest, with sixteen ethylene glycol units (PEG-A), has its bulk located toward the middle of the plane containing the gramicidin dimers (Figure 5). The mid-section of PEG-A runs approximately perpendicular to the long axis of all dimers and is sandwiched between dimer AB and dimers EF and CD (the underscore indicates an adjacent asymmetric unit, see Figure 5). The polymer chain therefore forms important crystal contacts within the layers of the Type I crystal lattice. The oxygen of its ethylene glycol units hydrogen bonds extensively with the Ne of the indole side chains of Trp₉ and Trp₁₁ that extend away from the long axis of the intertwined double helices (Figure 5). Another two PEG molecules, with seven ethylene glycol units each (PEG-B, PEG-B'), are located close to the C-terminus of gramicidin chain A. They create crystal contacts between layers in the crystal lattice by hydrogen bonding with Trp₁₅ of one layer and the ethanolamine cap of gramicidin from another layer. It is possible that PEG-B and PEG-B' derive from a single PEG chain but with poor electron density between the two they have been refined as separate entities. The maps for all three gramicidin structures reported in this work also show a sphere of electron density between PEG-B and PEG-B'. Modeling and refining this volume as water, ammonium or sodium resulted in B-factors that differ significantly from those of the surrounding atoms or resulted in improbable hydrogen bonding for a positively charged species. Because this density could not be reasonably fit it was left unmodelled. The last PEG with 2 ethylene glycol units (PEG-C) runs parallel to the long axis of dimer CD and is anchored by two hydrogen bonds to Trp₁₁ from chain D and a symmetry related chain F.

Of note is the observation that the resolution of the gramicidin structures solved in this study scales with the chain length of the MAG used to create the hosting mesophase. Thus, resolutions of 1.08, 1.26 and 1.70 Å were obtained in 7.7 MAG, 8.8 MAG and 9.9 MAG, respectively. In our hands, the shortest chain lipid, 7.7 MAG, generally produces data of the highest quality and resolution in separate *in meso* crystallization trials⁴⁰ (and unpublished data, J. Lyons, D. Aragão, T. Soulimane, M. Caffrey). While the number of instances is not great, this short chain MAG is generating structure-grade crystals where the default lipid, 9.9 MAG, is either not producing crystals or the crystals it does generate are of poor quality. It is not clear why 7.7 MAG is outperforming the other lipids. In addition to producing a thinner, less curved bilayer, it is more prone to forming the sponge phase. A looser, less strained bilayer characteristic of the sponge phase may favor the growth of bigger and better ordered crystals as has been speculated on previously.^{4,38}

3.2. Crystallization Mechanism

3.2.1. Three Hosting Lipids, One Crystal Form—An important finding of this work is that mesophases formed from three distinctly different MAGs go on to create identical crystals of gramicidin by the *in meso* method. Thus, at the level of crystal growth rate and final structure there was no measurable difference between the three hosting lipids. What made this study possible in the first place was the prior knowledge that all three lipids form the cubic phase when fully hydrated at or close to 20 °C. However, the bilayer thickness of the cubic phase is different in each with 7.7 and 9.9 MAG having the thinnest and thickest bilayers, respectively. The expectation was that this significant difference in microstructure

would influence the state of the gramicidin in the mesophase prior to crystallogenesis and, in turn, reflect itself as a different form in the resulting crystal. In this way then it was hoped to access crystallographically the HSH form of gramicidin which, to date, has only been characterized structurally by NMR.

The finding that all three lipids produced identical crystal structures was unexpected. To what then can we ascribe this result? One possibility is that the conformation of the peptide is set by the organic solvent (TFE) and the protocol used to prepare samples for reconstitution (Scenario 1, Table S3). Of note however is the controversial nature of any such solvent effect (see Sawyer et al.⁴¹ and Killian et al.⁴²). Presumably then if it is the DSDH form that gets reconstituted into the mesophase bilayer initially it does not, under current *in meso* crystallization conditions, equilibrate to other, perhaps more energetically preferred forms. As such, it is trapped in the mesophase as a DSDH which subsequently shows up in the final crystal.

Another explanation for how the same crystalline gramicidin conformation emerges is that the peptide actually reconstitutes into the cubic phase bilayer in the same DSDH conformation despite the large differences in mesophase microstructure (Scenario 2, Table S3). The DSDH form goes on then to nucleate during *in meso* crystallogenesis giving rise to identical final crystal structures in a manner that is independent of the hosting lipid. This is perhaps surprising given the large difference (6.5 Å comparing 7.7 MAG and 9.9 MAG)⁴⁰ in the bilayer thickness of the parent cubic phases which might be expected to influence the pitch of the DSDH, if not the overall conformational state of the peptide. But such conformational differences, if they exist in the starting mesophase, do not show up in the final crystal. This suggests that the DSDH form crystallized is a particularly stable conformation.

It is also possible that the three different MAGs used in this study generate distinct mesophases that support different gramicidin conformations as a prelude to crystallogenesis. In this scenario (Scenarios 3 and 4, Table S3) however, the DSDH form is the most stable conformation. Thus, during the processes that give rise to nucleation and crystal growth, those other forms (Footnote 2) convert uniformly to the DSDH conformation and it is this that appears in the final crystal. As a prelude to crystal formation the extant model includes an intermediate state where the proteins are locally concentrated and partially ordered in a lamellar domain.⁴ It is possible that the conversion to the DSDH happens in this more fluid environment (Scenario 5, Table S3).

This discussion highlights the need for follow up studies to establish the effect that different solvents and dispersants, and indeed reconstitution protocols, have on the conformation that exists when gramicidin is incorporated into the lipidic cubic phase of MAGs. This should then be related to the form that ultimately crystallizes by the *in meso* method. Assorted spectroscopic, scattering and chromatographic methods might be used to advantage here.

3.2.2. A Role for PEG—In addition to having the same structure in crystals grown from mesophases created using different lipids, the composition of the gramicidin crystal was almost identical in each case. Of particular note is the PEG component which was mapped to four regions of electron density. Two of these, represented by PEG-B and PEG-B', are located at the end of the DSDH where the planar sheets of gramicidin come together in the

Footnote 2: In a separate study using circular dichroism we obtained evidence that gramicidin exists in the HSH form when reconstituted into the bilayer of the cubic phase.²³ However, in that study a different reconstitution protocol was used which involved dissolving the peptide directly in the molten lipid. Thus, the peptide was not exposed to solvent as was the case in the current study. As noted, exposure to solvent may have an effect on the conformation adopted by gramicidin and so a direct comparison between the two studies is not appropriate.

Type I packing arrangement. This corresponds to the interfacial region of the lipid bilayer in the mesophase from which crystals grew and, as a consequence, are not unexpected. However, the third and longest PEG molecule, PEG-A, resides in an elongated state with the bulk of its mass at the center of and in the plane containing the DSDH. It passes in between gramicidin dimers and hydrogen bonds with the Ne of tryptophan side chains extending from the long axis of the DSDH dimers. To understand how this long stretch of polymer might find its way to this location in the crystal lattice we must first consider the means by which crystals form by the *in meso* method.

As noted, a proposal has been advanced for how *in meso* crystallogenesis takes place at a molecular level (Figure 1).^{1,4} It begins typically with an isolated biological membrane which is treated with detergent to solubilize the target protein. The protein-detergent complex is purified by standard wet biochemical methods that usually involve a number of chromatographic steps. Homogenizing with a MAG effects reconstitution of the purified protein into the bilayer of the bicontinuous cubic phase. The protein retains its native conformation and activity and is free to move within the plane of the cubic phase bilayer. A precipitant is added to the mesophase which triggers a phase separation. Under conditions leading to crystallization one of the separated phases is lamellar and becomes enriched in protein. The locally high concentration of protein (that may or may not include detergent and native membrane lipid), in conjunction with an appropriate bathing solution composition and bilayer microstructure, act to facilitate nucleation and crystal growth. The growing crystal is fed by proteins moving through a lamellar portal to the face of the crystal from the bulk mesophase which acts as a protein reservoir. Experimental evidence exists in support of aspects of this hypothesis.^{1,4,43}

In the case of gramicidin, there is no solubilizing detergent and, given the purity of the peptide as purchased, it is unlikely to harbor any bound lipid. Thus, combining the dry lipid/gramicidin mix with water at 20 °C spontaneously generates the cubic phase with the peptide reconstituted in its bilayer.²³ What probably happens then as soon as the precipitant makes contact with the gramicidin-laden mesophase is that it experiences an osmotic shock.⁴ This is so because the mesophase itself is porous and permeated by water-filled channels whilst the precipitant is a concentrated solution of high molecular weight PEG. The osmotic shock itself may trigger a local and transient dehydration of the mesophase bolus which, if severe enough, could stabilize the lamellar phase.⁴⁴ With time, the precipitant components make their way into the recesses of the mesophase bolus and the osmotic shock dissipates. As the concentration of PEG in the mesophase rises it induces a cubic-to-sponge phase transition. The sponge phase is characterized by enlarged aqueous channels and a less ordered mesophase characterized by diffuse X-ray scattering.³⁸ However, the sponge phase retains the character of being bicontinuous and thus, can support crystal growth by the mechanism outlined above for the *in meso* method. The proposal that the sponge phase forms during crystallogenesis is supported by the observation that, with time in contact with the precipitant, the mesophase adopted a more fluid character reminiscent of the sponge phase. In fact, it is from the fluid sponge phase that crystals were harvested.

PEG is a water-soluble, linear polymer composed of repeating ethylene glycol (-CH₂-CH₂-O-) units. Presumably, it enters the mesophase by way of its aqueous channels which are continuous with the bulk medium, in this case, the precipitant solution. The channels, which start out quite narrow - just tens of ångströms wide - are surrounded by a highly curved bilayer of MAG. Thus, the wall of the channel is coated with polar lipid head groups made up of glycerols and ester moieties. With distance from the core of the aqueous channel the polar interface gives way to the apolar hydrocarbon of the bilayer created by the acyl chains of the MAG. In this environment the PEG polymers reptate through the channels to the core of the mesophase bolus in a process driven by diffusion and mass action. Within the

confines of the mesophase, the PEG molecules are expected to partition preferentially at the interface that separates the aqueous core of the channel and the apolar interior of the lipid bilayer. There, the apolar methylenes of the ethylene glycol units orient toward the hydrophobic interior of the bilayer. Its ether oxygen point toward the core of the aqueous channel where it can hydrogen bond with glycerol hydroxyls and water at the interface. In so doing, PEG has the effect of expanding the area per lipid molecule at the interfacial region, thereby lessening curvature and stabilizing the more swollen sponge phase variant of the mesophase.

The current crystallization study was carried out at a MAG:gramicidin mole ratio of 20:1. Assuming that the peptide and lipid are uniformly distributed within the bilayer of the mesophase upon reconstitution then, on average, each gramicidin DSDH dimer will be surrounded by 1 to 2 annuli of lipid molecules. As PEG polymers contact and enter the mesophase they will very quickly encounter and begin to interact with gramicidin. The interactions between gramicidin and PEG, revealed in the *in meso* crystal structure (Figure 5), likely reflect the kind of interactions that occur in the mesophase prior to crystallization. Thus, the ether oxygens of PEG at the aqueous/bilayer interface establish hydrogen bond contact with the Ne of tryptophan side chains extending from the DSDH dimers at that same interface. (This scenario assumes that gramicidin has already adopted the DSDH conformation. We cannot however discount the possibility that PEG triggers a transition to the double stranded form.) In the DSDH, eight tryptophans from the two gramicidin monomers are arranged relatively uniformly along the long axis of the dimer. Trp₁₅ is closest to the interface and likely is the first tryptophan to be encountered by PEG as it moves into the aqueous channels of the mesophase. Because of their close proximity to one another in the PEG chain it is possible that adjacent ethylene glycol units bring DSDH dimers together. In so doing, the local concentration of gramicidin rises further, facilitating nucleation and crystal growth.

Trp₁₃, Trp₁₁ and Trp₉ are arrayed on the DSDH dimer along and around its long axis in the direction away from the interface deeper into the hydrocarbon core of the bilayer. Thus, PEG has the opportunity to move from Trp₁₅ at the interface and to penetrate deeper into the apolar recesses of the bilayer where it can interact with other tryptophans. Presumably, Trp₁₃ is the first candidate donor followed, in turn, by Trp₁₁ and Trp₉. In fact, the polymer may choose to traverse the entire bilayer hopping from Trp₁₅ on one monomer in one leaflet of the bilayer all the way across via the intervening six tryptophans to Trp₁₅ on another monomer in the adjacent leaflet of the bilayer.

Hydrogen bonding to the Ne of buried tryptophans would enable the relatively polar ether oxygen of PEG to partition into the apolar interior of the bilayer. At the same time, the methylenes of individual ethylene glycol units would likely orient in such a way as to interact favorably with similar moieties of the lipid acyl chains which abound in the bilayer interior. In this way then it is possible to explain how PEG, as a water-soluble polymer, can make its way into the low dielectric interior of the mesophase bilayer facilitated by the presence of the transmembrane gramicidin dimer. The fact that PEG-A is found in the crystal with 60% of its 16 modeled ethylene glycol units at the mid-plane of the layered gramicidin molecules undoubtedly reflects a set of polymer-peptide interactions that are particularly favorable energetically (Figure 5).

In a separate study, we demonstrated that high concentrations of gramicidin in the cubic phase of 9.9 MAG induced formation of the inverted hexagonal (H_{II}) phase.²³ This was explained by a hydrophobic mismatch between the presumed HSH form of the peptide *in meso* and the bilayer in which it resided. It was speculated further that locally high concentrations of the peptide that must exist prior to nucleation and crystal growth by the *in*

meso method would work against crystal growth by favoring H_{II} phase formation. This led to the suggestion that additives and/or hosting lipids which stabilize a flatter, less curved aqueous/apolar interface would facilitate crystallization. This is entirely consistent with the results presented in the current study. PEG, the common precipitant ingredient in all three hosting lipids examined, induced a sponge phase with these same characteristics and it is in its presence that structure-quality crystals of gramicidin formed. It is possible then by flattening out the bilayer interface of the cubic mesophase that PEG creates an environment that preferentially stabilizes the DSDH form of gramicidin. The latter has a more cylindrical shape in contrast to the HSSH conformation which is hourglass shaped (Figure 2). A flatter, more lamellar bilayer is likely to accommodate a cylindrical object with its long axis parallel to the bilayer normal more so than one that necks down towards its mid-section. Thus, it may be that by stabilizing the sponge phase the PEG component of the precipitant favors conversion to the DSDH form which ends up in the final crystal (Scenario 4, Table S3). Any difference in the original conformation that might exist upon reconstitution may well disappear upon equilibration of the hosting mesophase with a PEG-containing precipitant.

This reasoning suggests that, in addition to examining the conformational state of gramicidin in the lipidic cubic phase as a prelude to crystallogenesis,²³ it is equally important to make such measurements after precipitant has been added. Thus, the gramicidin might exist in different states depending on the hosting lipid but then transition to another upon treatment with PEG (Scenario 3, Table S3). The presence of PEG, and the sponge phase it induces, may selectively stabilize the DSDH form. This can only be established by following the conformational state, and indeed mesophase characteristics, from initial reconstitution into the lipidic cubic phase all the way to sponge phase formation on to nucleation and crystal growth.

3.2.3. An Alternative Crystallization Mechanism?—The above discussion is based on the premise that gramicidin crystallizes from the lipidic mesophase by the so-called *in meso* mechanism as already described (Figure 1). However, since gramicidin is soluble in pure PEG, we must be open to the possibility that gramicidin is crystallizing from the lipidic mesophase by some other mechanism that involves dissolution in PEG. The following observations are presented that argue against this possibility. The current *in meso* crystallization trials were performed using water-based precipitant solutions containing high molecular weight PEGs at 20 to 30 % (w/w). Separately, we have established that gramicidin has a very low solubility (micromolar solubility, Table S1) in the PEG-containing precipitant solutions that produced diffraction-grade crystals. It is hard to visualize how such an apolar peptide as gramicidin would partition preferentially out of the bilayer of the mesophase into the bathing precipitant solution and to crystallize therein. Second, all crystals were observed to grow within the confines of the mesophase, not in the precipitant solution. Third, gramicidin crystals produced in this study exhibit Type I or layered packing which is entirely consistent with the *in meso* crystallization mechanism.

3.3. Crystallizing ‘Small Proteins’ *In Meso* is Worthy of Consideration—

Arguments have been advanced as to why the original cubic phase method would not work with proteins having fewer than five transmembrane helices.⁴⁵ The first has to do with the thermodynamic driving force which accrues from having proteins aggregate at regions of minimum curvature - the center of the so-called monkey saddle - within the unit cell of the cubic phase (Figure 1). In so doing, the aggregate stabilizes and helps propagate a local lamellar phase where the hydrophobic mismatch between the apolar surface around the mid-section of the protein and the bilayer interior is lessened. Calculations performed using the cubic-Pn3m phase formed by 9.9 MAG at 20 °C show that the elastic energy component of the chemical potential driving crystallization is dependent on membrane protein radius (in the plane of the bilayer) to the fourth power. Thus, proteins with a tight cluster of four or

less idealized transmembrane α -helices will not release enough energy upon aggregating to compensate for the energy costs associated with nucleation and crystal growth. The second factor working against nucleation in this theoretical model is the energy barrier that must be crossed as proteins move between monkey saddle centers separated from one another by horse saddles where curvature is maximized (Figure 1). This barrier serves to slow the overall process of protein aggregation and ultimately crystal growth.

In this and a related¹⁷ study, we show that gramicidin crystallizes *in meso* and that the crystals formed using three different hosting lipids, including 9.9 MAG, are of structure-quality. Gramicidin is not a protein, it is a peptide with 15 residues. Nonetheless, it has many of the attributes of a small protein and has been referred to as a mini-protein.⁴⁶ Under current experimental conditions, it is long enough, at 35 Å, to cross the membrane, not as an idealized α -helix, but as a DSDH with a radius in the plane of the membrane of ~18 Å. According to the model calculations of Grabe et al.⁴⁵ referred to above this DSDH should not crystallize *in meso* because its cross-sectional area, and thus its perimeter, in the plane of the membrane is simply too small. The disparity between the theoretical analysis of Grabe et al.,⁴⁵ and our finding that gramicidin, as a mini-protein, does indeed crystallize *in meso* can be explained as follows. To begin with, the calculations are based on an idealized cubic-Pn3m phase formed by 9.9 MAG at 20 °C. Under these conditions, the bilayer of the cubic phase is indeed highly curved and the energetics described by Grabe et al.,⁴⁵ apply. However, the conditions under which gramicidin crystallized *in meso* included a precipitant with a high PEG concentration. As noted, PEG stabilizes the sponge phase which, like the cubic mesophase from which it forms, is bicontinuous. Accordingly, it can support crystallization in a manner entirely consistent with the proposed *in meso* mechanism but with energy barriers that are less than those expected for the simple cubic-Pn3m phase. In the sponge phase overall curvature is considerably reduced. Thus, the magnitude of the elastic energy term referred to above that counters the crystallization of smaller proteins is lessened. Additionally, the aqueous channels of the sponge phase are considerably enlarged compared to the default cubic-Pn3m phase, and the sponge phase itself is less ordered (as judged by small-angle X-ray scattering³⁸) and more fluid. Thus, the horse saddle regions, which in the cubic-Pn3m phase have high curvature energy, are less curved. Accordingly, the energy barrier experienced by proteins moving throughout the sponge phase is less. This, in turn, enables a more rapid onset of nucleation and crystallogenesis.

On thermodynamic and kinetic grounds therefore, crystallization of small proteins should be possible by the *in meso* method when the conditions are favorable. The screening process is designed to sample a wide variety of chemical and environmental conditions that adjust the character of the hosting mesophase and the target protein. When the proper conditions are found, crystals should form.

3.4. Functional Significance of the DSDH

Regardless of the lipid used to create the hosting mesophase for *in meso* crystallization of gramicidin, the DSDH was the only conformation observed in this study. Further, the pitch of the helix was sufficiently large that ions could not pass through the core of the dimer. Accordingly, it was the non-conducting or closed form of the dimer that was found.

One of the assumptions to explain this result is that the crystals responsible for these structures nucleated from lamellar domains of gramicidin within the mesophase and, by extension, represent growth from a membrane mimetic. This suggests therefore that the DSDH form of the peptide found in the crystal is a conformation that might exist in a biological membrane. Energetically, this is not expected to be a preferred conformation because several of the tryptophan indole side chains are buried in the bilayer interior. However, the energy cost of so positioning indoles is context dependent.⁴⁷ In this case, the

four tryptophans at alternating positions in the C-terminal half of the peptide have highly apolar leucine or valine residues as nearest neighbors (see Section 1). To some degree, these would facilitate indoles residing in an apolar environment. It is possible too that the DSDHs associate to form multimers. Through cation- π interactions⁴⁸ between tryptophans of adjacent dimers stabilization of the intertwined form in a bilayer setting could be envisioned. The other alternative is that the DSDH conformation was induced to form and was stabilized by PEG in the precipitant solution, as described.

4. Conclusions

In this study, three different MAGs were used to create hosting mesophases with different microstructures in which to crystallize linear gramicidin by the *in meso* method. In all three cases, crystals with the same space group and unit cell metrics and virtually identical peptide structures were observed. The asymmetric unit contained a trimer of dimers in the non-conducting, antiparallel, left-handed DSDH conformation. This result was a surprise in light of the expectation that a different mesophase microstructure would stabilize different conformations of the peptide that would eventually crystallize by the *in meso* method. The finding has been rationalized in several ways. One posits that the DSDH is the form that gets reconstituted as dictated by the sample preparation materials and methods and that this persists into the crystal. Another suggests that the preferred state in all three mesophases is the DSDH which is the form that crystallizes. Yet another considers that the peptide conformation is indeed different in the different mesophases but that conversion to the DSDH form happens during the crystallization process, aided directly or indirectly by PEG in the precipitant. Finally, it is possible that the transition does not occur until the protein locally concentrates in a partially ordered lamellar domain that subsequently produces crystals.

All of the conditions that produced *in meso* crystals of gramicidin in the three different MAGs included PEG. And in all cases, the sponge phase was observed to form during incubation likely attributable to the presence of the polymer. PEG is seen clearly as part of all three crystal structures. It has subsequently been speculated to play a role in locally concentrating the peptide within the mesophase thereby facilitating nucleation and crystal growth in a way that is independent of MAG type. PEG is also seen to form stable, non-ionic interactions with gramicidin involving, in particular, the indole side chain of tryptophan. It is possible that PEG-mesophase and PEG-peptide interactions dictate the final form of gramicidin seen in crystals formed by the *in meso* method.

It is apparent that to more fully understand the mechanism of gramicidin crystallization in the current *in meso* system a more complete examination of the state of the peptide throughout the process is required. Thus, spectroscopic, chromatographic and scattering methods might usefully be brought to bear on the peptide conformation in solution prior to reconstitution, in the mesophase immediately upon reconstitution and following the addition of precipitant, on into the partially ordered and the final crystalline state.

In the course of this study, we have entertained the possibility that gramicidin crystallizes by a mechanism other than that proposed for the *in meso* method; one that involves dissolution in PEG. This has been discounted based on the measured low solubility of the peptide in PEG-containing solutions and the Type I or layered packing observed in grown crystals that are more consistent with the extant *in meso* mechanism.

The fact that the DSDH form of gramicidin is what grew by the *in meso* crystallization method might suggest that this conformation is physiologically relevant. This is based on the reasoning that crystallization takes place from a lipid bilayer which is a reasonable

membrane mimetic. It is also possible that other conformational states exist in the mesophase prior to the addition of precipitant and crystallization. A proposal for how conversion to and crystallization of the DSDH form occurs *in meso* has been presented.

The gramicidin used in this study is from a commercial, highly purified source. It is devoid of detergents and membrane lipids, amphipathic molecules that often accompany membrane proteins into crystallization trials. Indeed, a role for both in the *in meso* crystallization process has been proposed.^{1,4} Bacteriorhodopsin has been crystallized by the *in meso* method beginning with purple membrane which does not have added detergent. However, this preparation comes with an abundance of lipids from the inner membrane of *Halobacterium salinarum*. In the case of gramicidin however, neither detergent nor lipids are present but structure quality crystals have been produced. In this instance therefore *in meso* crystallization occurs in the absence of adventitious lipid and detergent.

The membrane mimetic used in the current study was composed of one of three different MAGs which are not common components of cellular membranes. Of note is the fact that 9.9 MAG (monoolein) was used in combination with an alkane to create black lipid membranes for early work on the ion conducting properties of gramicidin.⁴⁹

That gramicidin, a relatively short peptide, crystallizes readily *in meso* and in a number of different lipids suggests that the method is applicable to smaller membrane proteins. Theoretical calculations had indicated that the method, in its original form, would not work with proteins having fewer than five transmembrane helices. But the method relies upon screening for conditions that adjust the microstructure of the mesophase and the character of the protein such that crystallization becomes possible even for smaller proteins. As a result, the method should find application with other low molecular weight membrane proteins many hundreds of which are coded for in the human genome.⁵⁰ And based on the findings in this and a related study,⁵¹ 7.7, 8.8 and 9.9 MAGs should find application in establishing conditions for growing structure quality crystals of these important targets.

Supplementary Material

Refer to Web version on PubMed Central for supplementary material.

Acknowledgments

The authors thank V. Cherezov and V. Pye for assistance with data collection and processing, and for helpful discussions. T. Smyth and J. Lee (University of Limerick) are gratefully acknowledged for advice on and support of the MAG synthesis project. This work was supported by grants from Science Foundation Ireland (07/IN.1/B1836), FP7 COST Action CM0902 and the National Institutes of Health (GM75915 (MC), P50GM073210 (RMS)). DA is supported by a Marie Curie Intra-European Fellowship (PIEF-GA-2009-235612). Diffraction data were collected at the GM/CA-CAT beamline, Advanced Photon Source. Use of the APS is supported by the US Department of Energy (DE-AC02-06CH11357). GM/CA-CAT is funded by the US National Institutes of Cancer (Y1-CO-1020) and General Medical Sciences (Y1-GM-1104).

References

1. Caffrey M. *Annu. Rev. Biophys.* 2009; 38:29–51. [PubMed: 19086821]
2. Raman P, Cherezov V, Caffrey M. *Cell. Mol. Life Sci.* 2006; 63:36–51. [PubMed: 16314922]
3. Anderson DM, Gruner SM, Leibler S. *Proc. Natl. Acad. Sci. U. S. A.* 1988; 85:5364–5368. [PubMed: 3399497]
4. Caffrey M. *Cryst. Growth Des.* 2008; 8:4244–4254.
5. Brakke K. *Experiment. Math.* 1992; 1:141–165.
6. Townsley LE, Tucker WA, Sham S, Hinton JF. *Biochemistry.* 2001; 40:11676–11686. [PubMed: 11570868]

7. Urry DW. Proc. Natl. Acad. Sci. U. S. A. 1971; 68:672–676. [PubMed: 5276779]
8. Veatch WR, Stryer L. J. Mol. Biol. 1977; 117:1109–1113. [PubMed: 606835]
9. Burkhart BM, Gassman RM, Langs DA, Pangborn WA, Duax WL. Biophys. J. 1998; 75:2135–2146. [PubMed: 9788907]
10. Cotten M, Fu R, Cross TA. Biophys. J. 1999; 76:1179–1189. [PubMed: 10049303]
11. Olczak A, Glowka ML, Szczesio M, Bojarska J, Wawrzak Z, Duax WL. Acta Crystallogr. Sect. D. 2010; 66:874–880. [PubMed: 20693686]
12. Olczak A, Glowka ML, Szczesio M, Bojarska J, Duax WL, Burkhart BM, Wawrzak Z. Acta Crystallogr. Sect. D. 2007; 63:319–327. [PubMed: 17327669]
13. Burkhart BM, Li N, Langs DA, Pangborn WA, Duax WL. Proc. Natl. Acad. Sci. U. S. A. 1998; 95:12950–12955. [PubMed: 9789021]
14. Glowka ML, Olczak A, Bojarska J, Szczesio M, Duax WL, Burkhart BM, Pangborn WA, Langs DA, Wawrzak Z. Acta Crystallogr. Sect. D. 2005; 61:433–441. [PubMed: 15805598]
15. Doyle DA, Wallace BA. J. Mol. Biol. 1997; 266:963–977. [PubMed: 9086274]
16. Wallace BA, Ravikumar K. Science. 1988; 241:182–187. [PubMed: 2455344]
17. Höfer N, Aragão D, Caffrey M. Biophys. J. 2010; 99:L23–L25. [PubMed: 20682243]
18. Chen Y, Tucker A, Wallace BA. J. Mol. Biol. 1996; 264:757–769. [PubMed: 8980684]
19. Lomize AL, Orekhov V, Arsen'ev AS. Bioorg. Khim. 1992; 18:182–200. [PubMed: 1376600]
20. Ketchum RR, Lee KC, Huo S, Cross TA. J. Biomol. NMR. 1996; 8:1–14. [PubMed: 8810522]
21. Caffrey M, Lyons J, Smyth T, Hart DJ. Curr. Top. Membr. 2009; 63:83–108.
22. Coleman BE, Cwynar V, Hart DJ, Havas F, Jakkam Madan Mohan, Patterson S, Ridenour S, Schmidt M, Smith E, Wells AJ. Synlett. 2004; 8:1339–1342.
23. Liu W, Caffrey M. J. Struct. Biol. 2005; 150:23–40. [PubMed: 15797727]
24. Cheng A, Hummel B, Qiu H, Caffrey M. Chem. Phys. Lipids. 1998; 95:11–21. [PubMed: 9807807]
25. Caffrey M, Porter C. J. Vis. Exp. 2010; 45 <http://www.jove.com/index/details.stp?id=1712>.
26. Caffrey M, Cherezov V. Nat. Protoc. 2009; 4:706–731. [PubMed: 19390528]
27. Fischetti RF, Xu S, Yoder DW, Becker M, Nagarajan V, Sanishvili R, Hilgart MC, Stepanov S, Makarov O, Smith JL. J. Synchrotron Radiat. 2009; 16:217–225. [PubMed: 19240333]
28. Otwinowski Z, Minor W. Methods Enzymol. 1997; 276:307–326.
29. CCP4. Acta Crystallogr. Sect. D. 1994; 50:760–763. [PubMed: 15299374]
30. Matthews BW. J. Mol. Biol. 1968; 33:491–497. [PubMed: 5700707]
31. McCoy AJ, Grosse-Kunstleve RW, Adams PD, Winn MD, Storoni LC, Read RJ. J. Appl. Crystallogr. 2007; 40:658–674. [PubMed: 19461840]
32. Murshudov GN, Vagin AA, Dodson EJ. Acta Crystallogr. Sect. D. 1997; 53:240–255. [PubMed: 15299926]
33. Emsley P, Cowtan K. Acta Crystallogr. Sect. D. 2004; 60:2126–2132. [PubMed: 15572765]
34. Davis IW, Leaver-Fay A, Chen VB, Block JN, Kapral GJ, Wang X, Murray LW, Arendall WB 3rd, Snoeyink J, Richardson JS, Richardson DC. Nucleic Acids Res. 2007; 35:W375–W383. [PubMed: 17452350]
35. Lovell SC, Davis IW, Arendall WB 3rd, de Bakker PI, Word JM, Prisant MG, Richardson JS, Richardson DC. Proteins. 2003; 50:437–450. [PubMed: 12557186]
36. Vaguine AA, Richelle J, Wodak SJ. Acta Crystallogr. Sect. D. 1999; 55:191–205. [PubMed: 10089410]
37. Ramachandran GN, Sasisekharan V. Adv. Protein Chem. 1968; 23:283–438. [PubMed: 4882249]
38. Cherezov V, Clogston J, Papiz MZ, Caffrey M. J. Mol. Biol. 2006; 357:1605–1618. [PubMed: 16490208]
39. Michel H. Trends Biochem. Sci. 1983; 8:56–59.
40. Misquitta LV, Misquitta Y, Cherezov V, Slattery O, Mohan JM, Hart D, Zhalnina M, Cramer WA, Caffrey M. Structure. 2004; 12:2113–2124. [PubMed: 15576026]
41. Sawyer DB, Koeppe RE 2nd, Andersen OS. Biophys. J. 1990; 57:515–523. [PubMed: 1689593]

42. Killian JA, Prasad KU, Hains D, Urry DW. *Biochemistry*. 1988; 27:4848–4855. [PubMed: 2458757]
43. Cherezov V, Caffrey M. *Faraday Discuss*. 2007; 136:195–212. discussion 213–129. [PubMed: 17955811]
44. Qiu H, Caffrey M. *Biomaterials*. 2000; 21:223–234. [PubMed: 10646938]
45. Grabe M, Neu J, Oster G, Nollert P. *Biophys. J*. 2003; 84:854–868. [PubMed: 12547769]
46. Andersen OS, Koeppe RE 2nd, Roux B. *IEEE Trans. Nanobioscience*. 2005; 4:10–20. [PubMed: 15816168]
47. White SH, von Heijne G. *Annu Rev Biophys*. 2008; 37:23–42. [PubMed: 18573071]
48. Gallivan JP, Dougherty DA. *Proc. Natl. Acad. Sci. U. S. A*. 1999; 96:9459–9464. [PubMed: 10449714]
49. Hladky SB, Haydon DA. *Nature*. 1970; 225:451–453. [PubMed: 5411119]
50. Nugent T, Jones DT. *BMC Bioinformatics*. 2009; 10:159. [PubMed: 19470175]
51. Li D, Lee J, Caffrey M. *Cryst. Growth Des*. 2010 In press.
52. Misquitta Y, Caffrey M. *Biophys. J*. 2001; 81:1047–1058. [PubMed: 11463646]

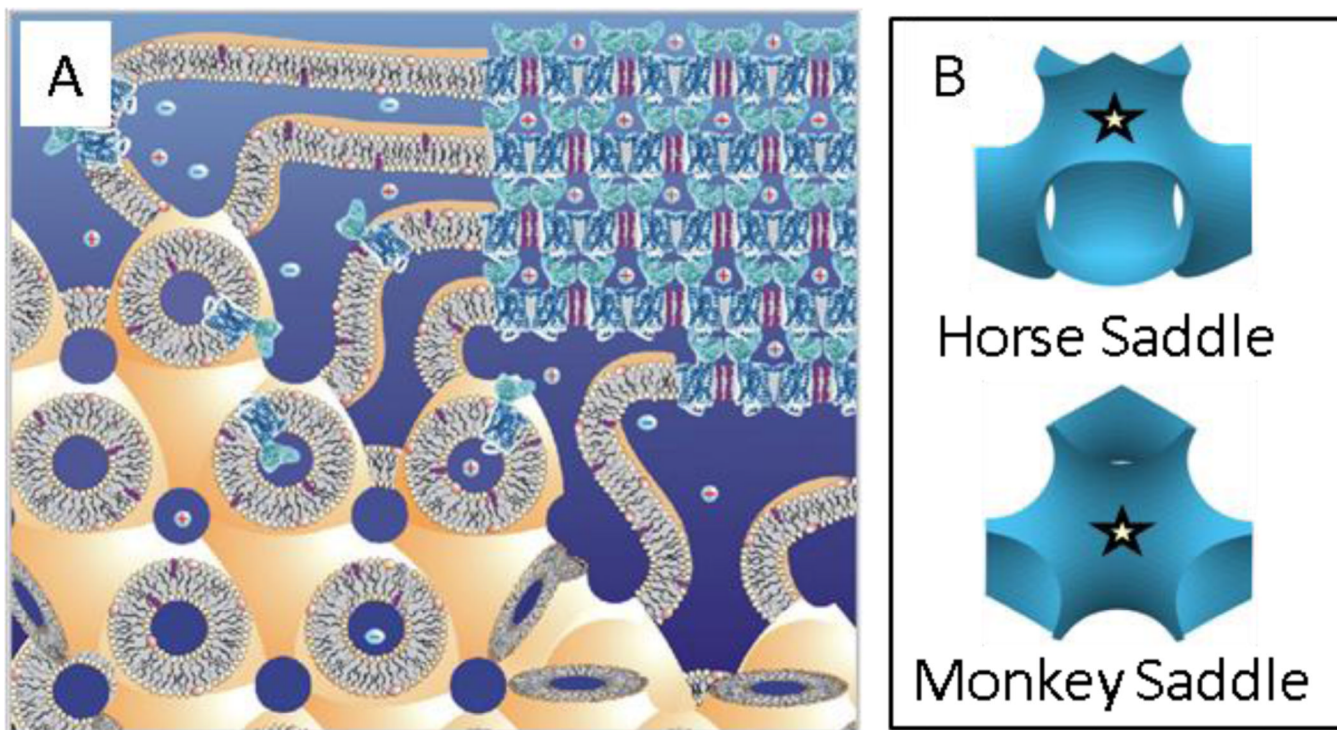


Figure 1.

The mesophases where *in meso* crystallization of membrane proteins takes place and topological features of the cubic mesophase. **A.** Schematic representation of the events proposed to take place during the crystallization of an integral membrane protein from the lipidic cubic mesophase. The process begins with the protein reconstituted into the highly curved bilayers of the bicontinuous cubic phase (bottom left quadrant). Added precipitants shift the equilibrium away from stability in the cubic membrane. This leads to phase separation, wherein protein molecules diffuse from the continuous bilayered reservoir of the cubic phase by way of a sheet-like or lamellar portal (upper left quadrant) to lock into the lattice of the advancing crystal face (upper right quadrant). Salt (positive and negative signs) facilitates crystallization, in part, by charge screening. Co-crystallization of the protein with native or added lipid (cholesterol) is shown in this illustration. As much as possible, the dimensions of the lipid (light yellow oval with tail), detergent (pink oval with tail), native membrane or added lipid (purple), protein (blue; β 2AR-T4L; PDB code 2RH1), and bilayer and aqueous channels (dark blue) have been drawn to scale. The lipid bilayer is approximately 40 Å thick. Panel taken from Caffrey.⁴ **B.** The periodic minimal surface of the cubic-Pn3m phase is shown in shades of blue and gray. Stars mark the location of the horse and monkey saddles referred to in the text. Surface generated with the program Surface Evolver.⁵

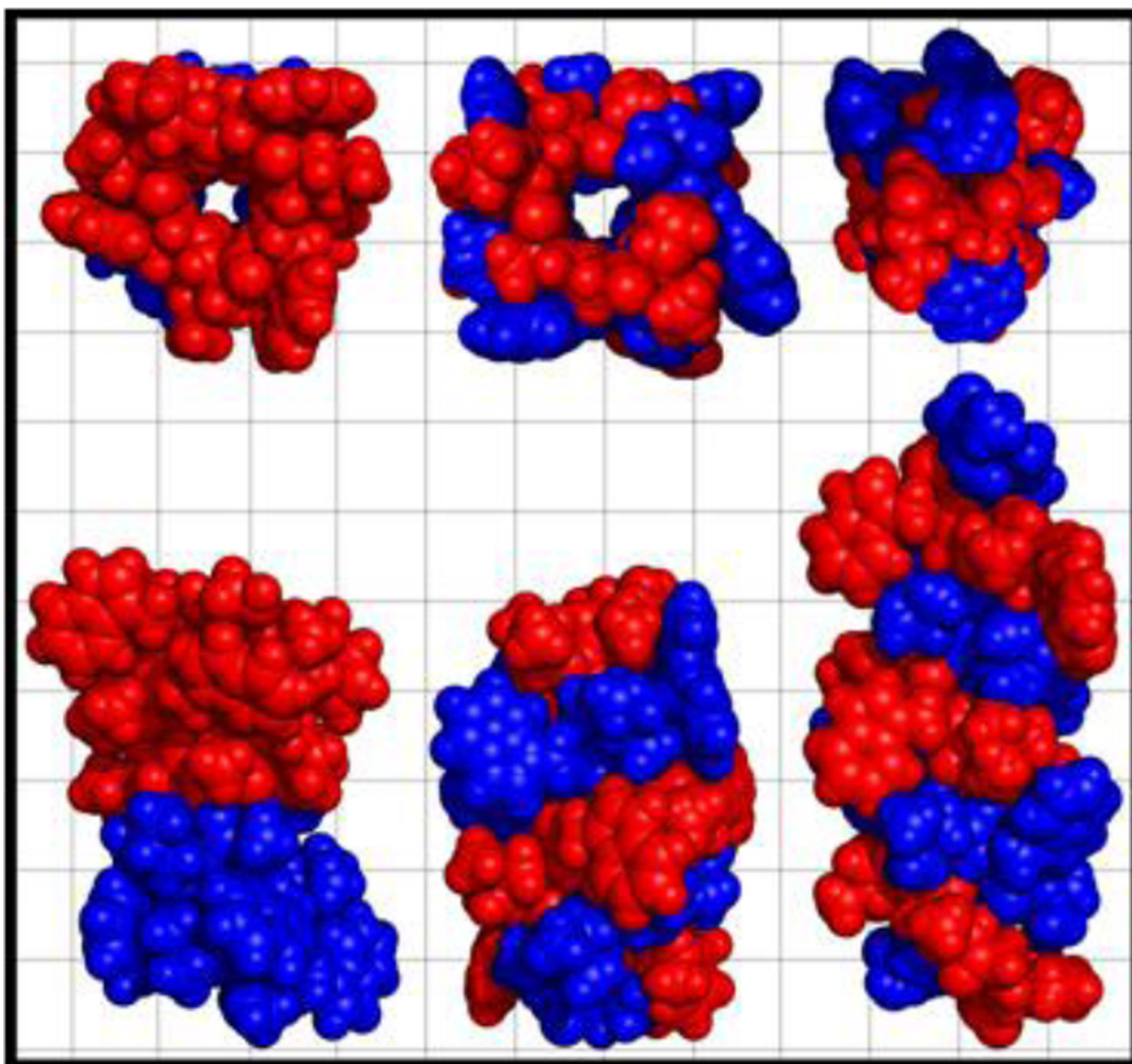


Figure 2. Conformations adopted by linear gramicidin. End on view along the normal to the membrane plane (upper panels). Side view from within the membrane (lower panels). The conformations shown include the HSHH (PDB ID, 1JNO; left panels), right-handed DSDH - ion bound form (PDB ID, 3L8L; center panels, ions not shown) and left-handed DSDH - non-ion bound form (PDB ID, 1ALZ; right panel). Individual monomers are colored red and blue for clarity. The background grid has vertical and horizontal lines every 5 Å for scale.

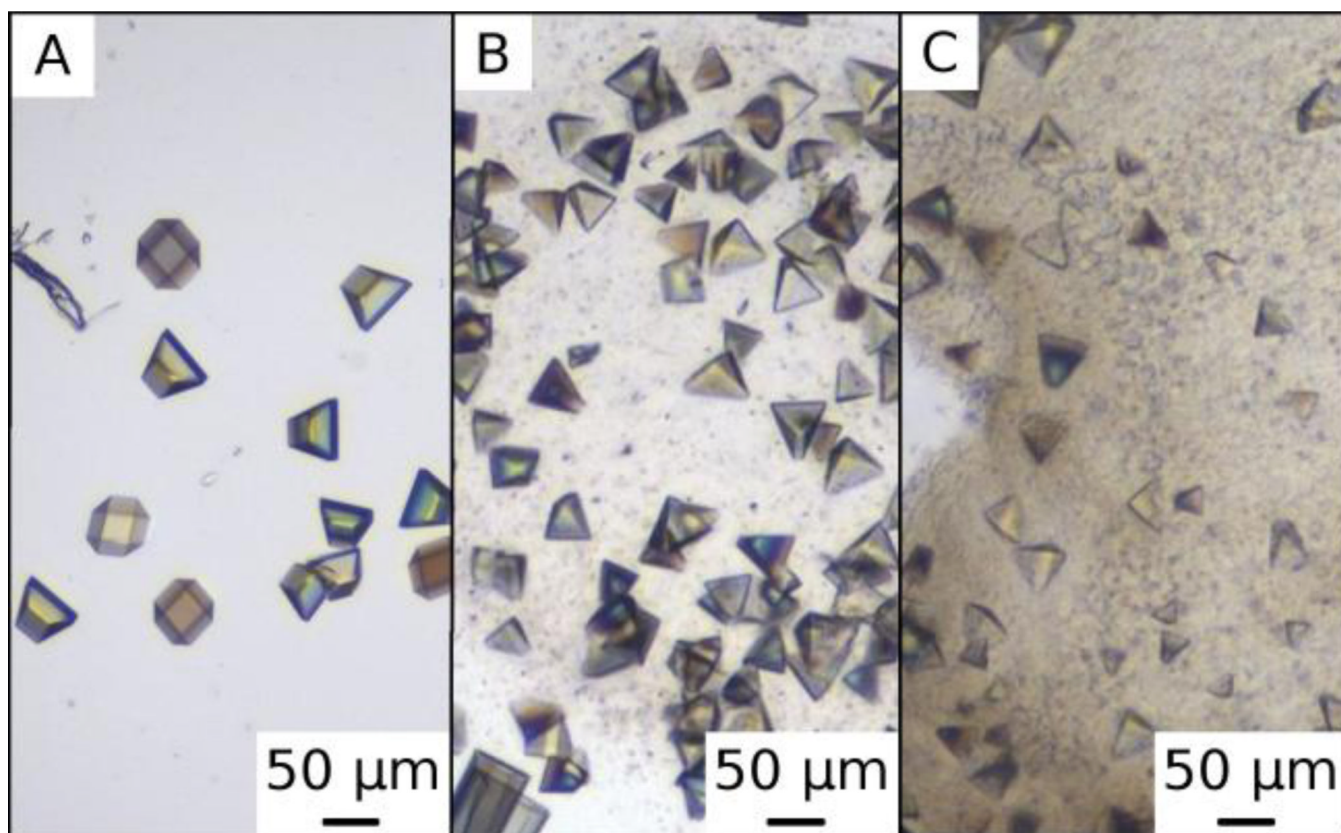


Figure 3. Crystals of gramicidin growing *in meso* using different hosting lipids. A) 7.7 MAG [28 % (w/w) PEG 2000 MME, 0.1 M Bis-Tris, pH 6.5], B) 8.8 MAG [30 % (w/v) PEG 8,000, 0.2 M NH_4SO_4], C) 9.9 MAG [20 % (w/v) PEG 6,000, 0.1 M Bicine, pH 9.0].

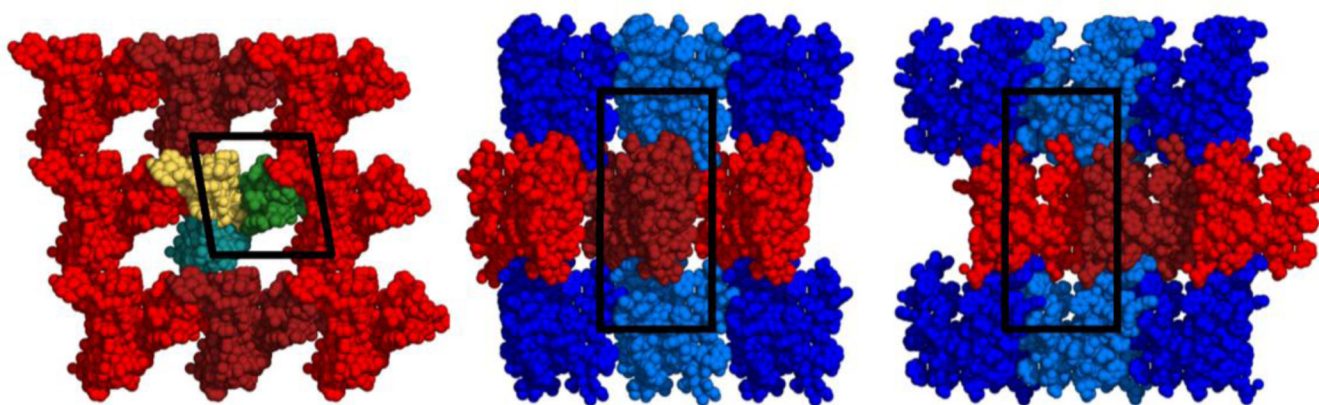


Figure 4. Layered (Type I) packing observed in crystals of gramicidin grown in the lipidic mesophase prepared with 7.7 MAG. Individual dimers are colored yellow, green and cyan (left panel). Alternate layers are colored red (light and dark) and blue (light and dark) to highlight Type I packing (center and right hand panels). The unit cell is boxed in black.

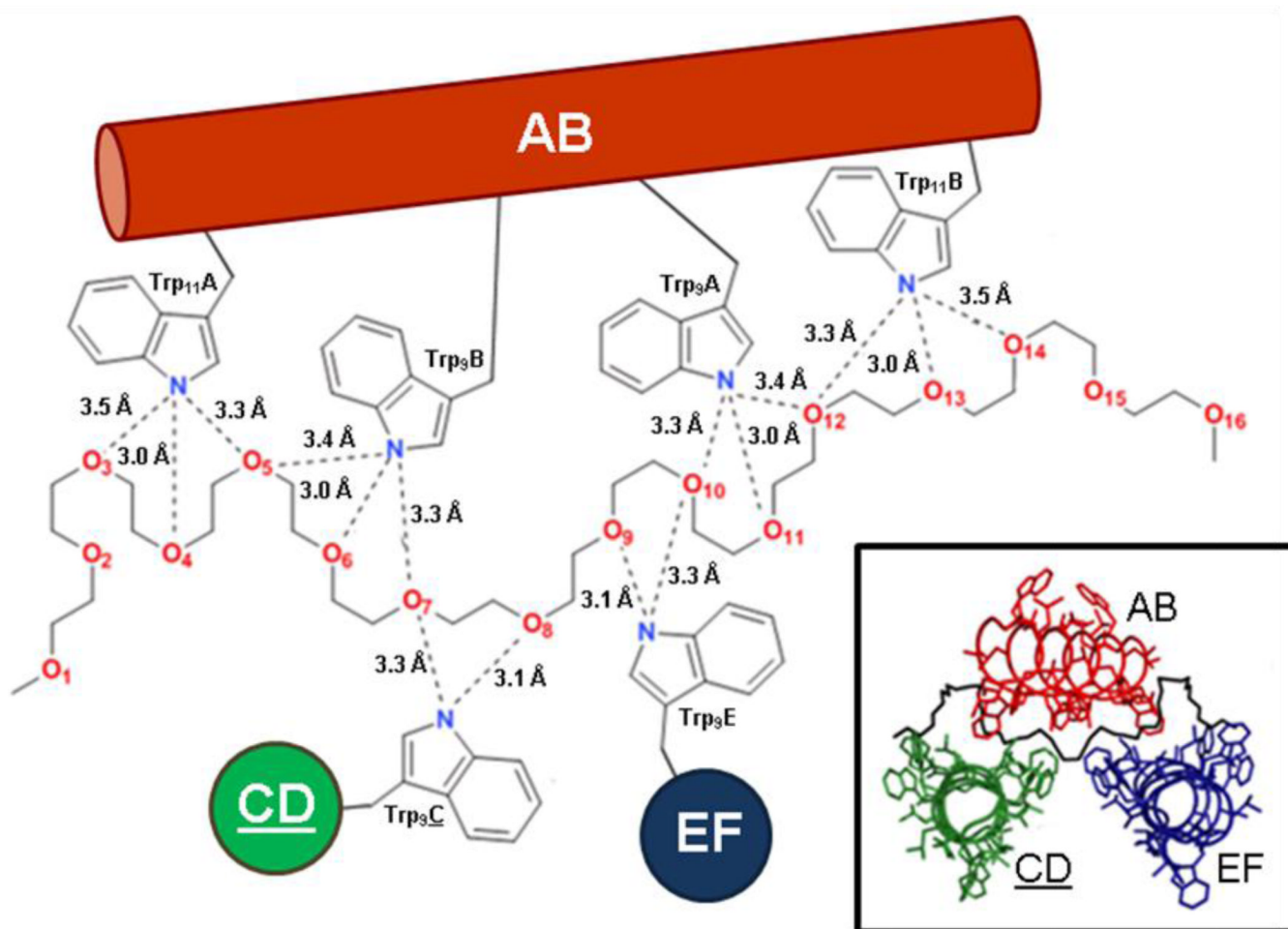


Figure 5. Schematic representation of hydrogen bonding (dashed lines) between oxygen atoms (red, the subscript identifies the ethylene glycol unit number) of PEG-A and tryptophan Ne atoms (blue) of gramicidin. Dimers AB (red cylinder) and EF (purple circle) derive from one asymmetric unit whilst dimer CD (green circle) is from an adjacent asymmetric unit. The inset shows dimers AB (red), EF (purple) and CD (green) in cartoon form with PEG-A in black stick representation. Crystals used for the structure shown were grown in the lipidic mesophase prepared with 7.7 MAG.

Table 1

Gramicidin structures available in the Protein Data Bank.

Method	Resolution (Å)	Dispersing Medium	PDB ID ^a
DSDH (AP ^b , RH ^c , ion-bound)			
MX	1.25	Methanol (+ NaI)	3L8L
MX	0.80	Methanol (+ KI)	2IZQ
MX	1.40	Methanol (+ CsCl)	1AV2
MX	1.70	Glacial acetic acid	1BDW
MX	1.14	Ethanol (+ RbCl)	1W5U
DSDH (AP ^b , LH ^d , ion-bound)			
MX	2.50	Methanol (+ KSCN)	1GMK
MX	2.00	Methanol (+ CsCl)	1C4D
DSDH (AP ^b , LH ^d , ion-free)			
MX	1.13	n-Propanol	1AL4
MX	0.86	Ethanol	1ALZ
MX	1.20	Methanol	1ALX
MX	1.70	LCP ^e , 9.9 MAG	2XDC
MX	1.28	LCP ^e , 8.8 MAG	PDBID
MX	1.08	LCP ^e , 7.7 MAG	2Y5M
DSDH (P ^f , LH ^d)			
NMR	n/a	Methanol (+ CaCl ₂)	1MIC
HSH (AP ^b , RH ^c)			
NMR	n/a	SDS micelle	1GRM
NMR	n/a	SDS micelle	1JNO
NMR	n/a	SDS micelle	1JO3
NMR	n/a	SDS micelle	1JO4
NMR	n/a	DMPC bilayer	1MAG
NMR	n/a	DDPC micelle	1NRU
NMR	n/a	DDPC micelle	1NRM

^a3L8L,¹¹ 2IZQ,¹² 1AV2,¹³ 1BDW,¹³ 1W5U,¹⁴ 1GMK,¹⁵ 1C4D,¹⁶ 1AL4,⁹ 1ALZ,⁹ 1ALX,⁹ 2XDC,¹⁷ 1MIC,¹⁸ 1GRM,¹⁹ 1JNO,⁶ 1JO3,⁶ 1JO4, and 1MAG²⁰

^bAP – anti-parallel.

^cRH – right-handed.

^dLH – left-handed.

^eLCP – lipidic cubic phase.

^fP – parallel.

Table 2

Diffraction data, refinement and model statistics for data sets 1 – 3

	Data set		
	1 ^a	2 ^b	3 ^c
Hosting lipid	7.7 MAG	8.8 MAG	9.9 MAG
Diffraction data ^d			
Space group	P2 ₁	P2 ₁	P2 ₁
Unit cell			
	a= 30.6 Å	a= 30.6 Å	a= 30.5 Å
	b= 62.8 Å	b= 62.8 Å	b= 62.6 Å
	c= 30.7 Å	c= 30.6 Å	c= 30.5 Å
	β= 100.0°	β= 100.0°	β= 100.0°
X-ray source	23ID-B,APS	23ID-B,APS	23ID-B,APS
Wavelength [Å]	0.83	0.98	1.03
Resolution limits [Å]			
Overall	1.08 – 30.20	1.26 – 31.40	1.70 – 31.30
Highest shell	1.08 – 1.09	1.26 – 1.29	1.70 – 1.74
No. of unique reflections	46,435	29,856	11,751
Completeness [%] ^c	95.0 (65.0)	96.4 (76.9)	94.2 (79.4)
Redundancy [%] ^c	6.3 (3.6)	7.1 (3.2)	3.0 (2.2)
R _{merge} [%] ^c	9.5 (41.8)	6.4 (27.9)	6.7 (26.5)
I/σ(I) ^c	15.8 (2.4)	22.6 (3.5)	13.1 (3.3)
Refinement model statistics ^c			
No. of reflections			
Working set	44,055 (2,238)	28,320 (1,670)	11,147 (706)
Test set	2,380 (132)	1,536 (94)	604 (29)
R _{factor} [%]	13.0	14.8	17.9
R _{free} [%]	15.5	16.9	21.4
Protein atoms	816	816	816
Solvent atoms	94	100	107
Average B-factor [Å ²]			
All atoms	14.0	14.7	20.3
Peptide	13.0	14.0	18.7
Chain A	11.5	12.4	16.9
Chain B	11.4	12.3	17.2
Chain C	12.8	13.6	18.4
Chain D	14.7	16.0	20.0
Chain E	12.8	13.6	18.7
Chain F	14.7	16.0	18.7
Solvent	22.9	24.9	33.0
PEG	22.6	24.9	32.8

	Data set		
	1 ^a	2 ^b	3 ^c
Water	31.5	25.9	40.0
Sodium Ion	-	-	48.7
R.m.s. deviations from ideal			
Bond lengths [Å]	0.02	0.02	0.02
Angles [°]	1.70	1.70	1.62

^aThis work, PDB ID - 2Y5M.

^bThis work, PDB ID - PDBID.

^cPDB ID - 2XDC.¹⁷

^dValues in parentheses are for the highest resolution shells